This is the author's version of an article that has been published in this journal. Changes were made to this version by the publisher prior to publication.
The final version of record is available at http://dx.doi.org/10.1109/TIP.2013.2283148

Metamer Mismatching

Alexander D. Logvinenko, Brian Funt, Christoph Godau

Note that the final published version does include several important updates.
If you would like a copy of the final version, simply mail to funt@sfu.ca

***Abstract*—A new algorithm for calculating the metamer mismatch volumes that arise in colour vision and colour imaging is introduced. Unlike previous methods, the proposed method places no restrictions on the set of possible object reflectance spectra. As a result of such restrictions, previous methods have only be able to provide approximate solutions to the mismatch volume. The proposed new method is the first to characterize precisely the metamer mismatch volume for any possible reflectance.**

***Index Terms*—Colour vision, metamerism, metamer mismatching, metamer set, metamer mismatch volume. EDICS: ELI-COL**

$\Phi = (\varphi_1, ..., \varphi_n)$	a set of sensors $(\varphi_1, ..., \varphi_n)$
$\varphi_i(x)$	i^{th} sensor response to spectral reflectance function $x(\lambda)$
$\Psi = (\psi_1, ..., \psi_n)$	a set of sensors $(\psi_1, ..., \psi_n)$
$\psi_i(x)$	i^{th} sensor response to spectral reflectance function $x(\lambda)$
Υ	concatenated set of sensors $(\varphi_1, ..., \varphi_n, \psi_1, ..., \psi_n)$
$r_i(\lambda)$	spectral sensitivity of i^{th} sensor
$p(\lambda)$	illuminant spectral power distribution
$\mathcal{X}$	set of all spectral reflectance functions
$\Phi : \mathcal{X} \to \mathbf{R}^n$	colour signal map
$\Upsilon : \mathcal{X} \to \mathbf{R}^{2n}$	colour signal map
$\Phi(\mathcal{X})$	object colour solid (i.e., the Φ-image of $\mathcal{X}$)
$\Upsilon(\mathcal{X})$	object color solid (i.e., the Υ-image of $\mathcal{X}$)
$\partial\Upsilon(\mathcal{X})$	boundary of the object color solid $\Upsilon(\mathcal{X})$
$x_{opt}(\lambda)$	optimal spectral reflectance function
$O(\Upsilon)$	optimal reflectances of color signal map Υ
$x_m(\lambda; \lambda_1, ..., \lambda_m)$	elementary step function with transition wavelengths $\lambda_1, ..., \lambda_m$
$\mathcal{M}(\mathbf{z}_0; \Phi, \Psi)$	metamer mismatch volume induced by the Φ colour signal $\mathbf{z}_0$ for sensor sets Φ and Ψ
$\partial\mathcal{M}$	boundary of metamer mismatch volume $\mathcal{M}$
$\Phi^{-1}(\mathbf{z}_0)$	metamer set for the Φ colour signal $\mathbf{z}_0$ (i.e., the set of reflectances Φ-metameric to $\mathbf{z}_0$)

Table I
NOTATION

I. INTRODUCTION

TWO objects that look the same colour under one light can differ in colour under a second light. An important reason for the difference in perceived colour of the two objects under the second light is that although the tristimulus values of the two objects may be identical under the first light, it is possible that they differ under the second. In other words, they are metameric matches (i.e., invoke identical sensor response triplets) under the first light, but fail to match, and hence are no longer metamers, under the second. This phenomenon is called *metamer mismatching* [1].

If a colour under one light can become two colours under a second light, then it is natural to ask: What is the range of possible colours that might be observed under the second light? More specifically, given a tristimulus value under, say, CIE illuminant D65, what is the set of possible tristimulus values that could arise under, say, CIE illuminant A? This set has been proven to be a convex body[1] [2], and it is commonly known as the *metamer mismatch volume* [1]. In general, given the spectral power distributions of two illuminants and the tristimulus values of an object under one illuminant, the problem is to compute the metamer mismatch volume. It suffices to compute only the metamer mismatch volume boundary, because the body is completely specified by its boundary.

Metamer mismatch volumes are both of theoretical and practical importance. They are important in image processing for many reasons. For example, in camera sensor design it is well known that there is a trade-off between image noise and colour fidelity. Sensors whose sensitivity functions are not within a linear transformation of the human cone sensitivity functions will introduce error, but this error has been difficult to quantify. The size of the metamer mismatch volume induced by the change from cone to camera sensitivity functions is potentially a good measure of the error, but requires an accurate method for computing the metamer mismatch volumes of the sort proposed here. Metamer mismatch volumes are also relevant to the problem of color 'calibration,' often referred to as the colour correction problem. Again, because of the differences in cone versus camera sensitivities, there is no unique answer as to how RGB camera responses should be mapped to human cone respones or a standard colour space such as CIE XYZ. Urban et al. [3] and Finlayson et al. [4]–[6] have used characteristics such as the center of gravity of (approximate) metamer mismatch volumes as a means of improving colour correction.

Metamer mismatch volumes are also very important in defining the limits of both human and machine-based colour constancy. In the image processing field, the goal of computational colour constancy has been to provide colour descriptors that are independent to the incident illumination. With the method described here, Logvinenko et al. have shown serious metamer mismatching can be [7] and therefore how the issue of colour constancy needs to redefined [8]. Furthermore, in the related field of lighting design metamer mismatch volumes are also important. In particular, lights leading to the smallest mismatch volumes are naturally expected to yield the best colour rendering [9], [10]). All of these applications have been limited, until now, by the lack of a method for computing metamer mismatch volumes precisely.

In terms of theoretical importance, work on calculating mismatch volumes has a long history (for a review see, e.g., Wyszecki & Styles, 1982). Generally, previous methods have been based on generating metameric reflectances under one

[1]That is, a closed convex set such that it can be radially "inflated" to include any element of the ambient vector space.

Copyright (c) 2013 IEEE. Personal use is permitted. For any other purposes, permission must be obtained from the IEEE by emailing pubs-permissions@ieee.org.

This is the author's version of an article that has been published in this journal. Changes were made to this version by the publisher prior to publication.
The final version of record is available at http://dx.doi.org/10.1109/TIP.2013.2283148

illuminant and then evaluating their tristimulus values under a second illuminant, thus producing points lying within the mismatch volume. However, it remains an unsolved problem as to how to describe fully the set of all the reflectances metameric to a given one under some fixed illumination, and hence these methods do not completely specify the metamer mismatch volume. Instead, they generate a sampling of the infinite set of possible metameric reflectances without a clear understanding how the resulting sample represents the complete set of metameric reflectances. A key limitation of such an approach is that the accuracy of representing the mismatch volumes by the cluster of points obtained can be poor. Moreover, as the precise boundary of the mismatch volume remains unknown, there is no way to determine the true accuracy of the approximation. The situation only becomes worse when the reflectances are sampled from a finite-dimensional subset of the infinite dimensional set of all the reflectances [3], [11]. Of the methods proposed thus far, none directly describes the theoretical limits of the metamer mismatch volume. In other words, none provides the metamer mismatch volume's boundary.

In this report we investigate the boundary of the metamer mismatch volume from the formal point of view and then provide an algorithm for computing the metamer mismatch volumes for arbitrary, strictly positive illuminants and strictly positive sensor sensitivity functions[2], without placing any restrictions on the reflectances.

II. Metamer Mismatching Theory

Consider a set of *sensors* $\Phi = (\varphi_1, ..., \varphi_n)$, the response of each of which to a reflecting object with spectral reflectance function $x(\lambda)$ illuminated by a light with spectral power distribution $p(\lambda)$ is given by

$$\varphi_i(x) = \int_{\lambda_{\min}}^{\lambda_{\max}} x(\lambda)\, p(\lambda)\, r_i(\lambda)\, d\lambda \qquad (i = 1, ..., n), \quad (1)$$

where $[\lambda_{\min}, \lambda_{\max}]$ is the visible spectrum interval, and $r_i(\lambda)$ is the spectral sensitivity of the i-th sensor. The vector $\Phi(x) = (\varphi_1(x), ..., \varphi_n(x))$ of the sensor responses will be referred to as the *colour signal* produced by the sensor set Φ in response to $x(\lambda)$ illuminated by $p(\lambda)$. In the case of trichromatic human colour vision $n = 3$, and $r_1(\lambda), r_2(\lambda)$, and $r_3(\lambda)$ are the human spectral sensitivities known as *cone fundamentals* [12]. Alternatively, $r_1(\lambda), r_2(\lambda)$, and $r_3(\lambda)$ can be treated as the sensors' spectral sensitivity functions of a digital camera or similar device.

Different objects may happen to produce equal colour signals. Such objects are called *metameric*. Specifically, two objects with spectral reflectance functions $x(\lambda)$ and $x'(\lambda)$ are called metameric under the illuminant $p(\lambda)$ if they produce equal colour signals, that is, $\Phi(x) = \Phi(x')$. Object metamerism depends on the illuminant. If the illuminant $p(\lambda)$ is replaced by a different illuminant $p'(\lambda)$ the hitherto metameric objects may cease to be metameric. In other words, the former metamers may no longer match under the new illuminant. This phenomenon—metamers becoming non-metamers—is called *metamer mismatching* [1].

Metamer mismatching may also happen if the spectral sensitivity of the sensors changes. An illuminant change (i.e., replacing $p(\lambda)$ with $p'(\lambda)$) is, formally, equivalent to changing the spectral sensitivity functions of the sensors. As a consequence, we will consider the general situation when a set of abstract colour mechanisms $\varphi_1, ..., \varphi_n$ is replaced by a different set $\psi_1, ..., \psi_n$. The new set of colour mechanisms can be understood as the result of altering either the illuminant or the colour mechanisms' spectral sensitivities, or both. Metamer mismatching arising solely from a change in illuminant will be referred to as *illuminant-induced metamer mismatching*, while that arising solely from a change of colour mechanisms as *observer-induced metamer mismatching*.

The general case of metamer mismatching concerns a set of colour mechanisms, $\Phi = (\varphi_1, ..., \varphi_n)$, each member of which is thought of as a linear functional on the set $\mathcal{X}$ of all the spectral reflectance functions (i.e., $0 \leq x(\lambda) \leq 1$), that is, $\varphi_i : \mathcal{X} \to \mathbf{R}$, where $\mathbf{R}$ is the real line, and $i = 1, ..., n$. Every colour mechanism φ_i will be assumed to have the form as in (1):

$$\varphi_i(x) = \int_{\lambda_{\min}}^{\lambda_{\max}} x(\lambda)\, s_i(\lambda)\, d\lambda \qquad (i = 1, ..., n), \quad (2)$$

where $s_i(\lambda)$ is the spectral weighting function fully specifying the colour mechanism φ_i. For example, $s_i(\lambda)$ might amount to $p(\lambda)\, r_i(\lambda)$. Consider another set of colour mechanisms, $\Psi = (\psi_1, ..., \psi_n)$, with the spectral weighting functions $s'_1(\lambda), ..., s'_n(\lambda)$. We will assume that both sets of colour mechanisms are linearly independent, and that Φ and Ψ are not a linear transformation of one another.

Note that both Φ and Ψ can be considered as linear maps (referred to as *colour maps*) of the form: $\mathcal{X} \to \mathbf{R}^n$ where $\mathbf{R}^n$ is the arithmetic n-dimensional vector space. The sets of all colour signals, that is, $\Phi(\mathcal{X})$ and $\Psi(\mathcal{X})$, form convex bodies in $\mathbf{R}^n$ [2], which are usually referred to as *object-colour solids* [1].

Given an object $x_0 \in \mathcal{X}$, the Φ pre-image, $\Phi^{-1}(\Phi(x_0))$ (i.e., $\Phi^{-1}(\Phi(x_0)) = \{x \in \mathcal{X} | \Phi(x) = \Phi(x_0)\}$), of its colour signal $\Phi(x_0)$ is the set of all the objects metameric to x_0 (with respect to Φ), and is referred to as its metamer set. Generally, when this set of metameric objects $\Phi^{-1}(\Phi(x_0))$ is mapped by Ψ into the Ψ-object-colour solid, it will be spread into a non-singleton set. It is the resulting set that is referred to as the metamer mismatch volume. More formally, the Ψ-image of the set of the Φ-metamers, $\Psi(\Phi^{-1}(\Phi(x_0)))$ is called the metamer mismatch volume associated with x_0.

Given colour maps, $\Phi = (\varphi_1, ..., \varphi_n)$ and $\Psi = (\psi_1, ..., \psi_n)$, let us consider a map $\Upsilon : \mathcal{X} \to \mathbf{R}^{2n}$ such that $\Upsilon(x) = (\mathbf{z}; \mathbf{z}')$, where $\mathbf{z} = (\varphi_1(x), ..., \varphi_n(x))$ and $\mathbf{z}' = (\psi_1(x), ..., \psi_n(x))$. The corresponding object-colour solid $\Upsilon(\mathcal{X})$ is a convex body in $\mathbf{R}^{2n}$. The Φ-object-colour solid, $\Phi(\mathcal{X})$, is the z-projection of $\Upsilon(\mathcal{X})$:

$$\Phi(\mathcal{X}) = \{\mathbf{z} \in \mathbf{R}^n : (\mathbf{z}; \mathbf{z}') \in \Upsilon(\mathcal{X}), \quad \mathbf{z}' \in \mathbf{R}^n\}.$$

[2]We believe that this positivity constraint is not a serious limitation in practice since any illuminant or sensor function can be approximated by a strictly positive function as accurately as required.

Copyright (c) 2013 IEEE. Personal use is permitted. For any other purposes, permission must be obtained from the IEEE by emailing pubs-permissions@ieee.org.

This is the author's version of an article that has been published in this journal. Changes were made to this version by the publisher prior to publication.
The final version of record is available at http://dx.doi.org/10.1109/TIP.2013.2283148

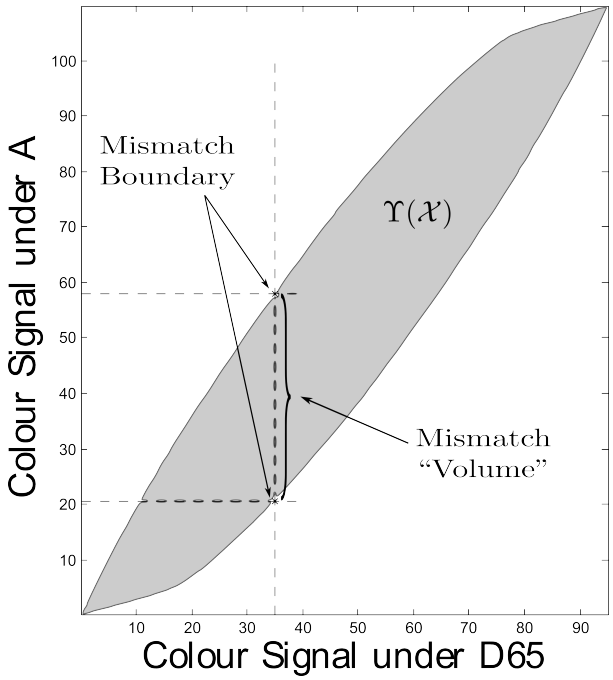

Figure 1. Illustration of the metamer mismatch volume for a monochromatic colour device based on CIE $\bar{x}(\lambda)$. The colour signals obtained under CIE illuminant $D65$ are plotted along the horizontal axis (z) , and under A along the vertical axis (z'). The shaded area indicates $\Upsilon(\mathcal{X})$, which is the set of all "colour" signal pairs arising under $D65$ and A from all possible object reflectances. The metamer mismatch volume boundary for colour signal value $z = 35$ under $D65$ is obtained from the projection to the z' axis of the cross-section (two points in this example) of $\Upsilon(\mathcal{X})$ defined by the intersection of the vertical line with the boundary of $\Upsilon(\mathcal{X})$. As can be seen from the figure, the colour signal $z = 35$ under $D65$ could, under A, potentially take on any value in the metamer mismatch volume $z' \in [20.5, 58]$.

Similarly, given an object $x_0 \in \mathcal{X}$ and its Φ colour signal $\mathbf{z}_0 = \Phi(x_0)$, the metamer mismatch volume $\Psi(\Phi^{-1}(\mathbf{z}_0))$ forms a cross-section of $\Upsilon(\mathcal{X})$; namely, $\{\mathbf{z}' \in \mathbf{R}^n : (\mathbf{z}_0; \mathbf{z}') \in \Upsilon(\mathcal{X})\}$.

To gain some intuition into metamer sets, metamer mismatch volumes, and why a metamer mismatch volume corresponds to a cross-section of the $\Upsilon(\mathcal{X})$-object-colour solid, consider the one-dimensional case of a pair of colour mechanisms φ_1 and ψ_1. In this case, the colour maps become simply $\Phi = (\varphi_1)$ and $\Psi = (\psi_1)$, and the object-colour solid $\Upsilon(\mathcal{X})$ becomes a convex region in 2-dimensions as shown in Figure 1.

For Figure 1 the CIE 1931 $\bar{x}(\lambda)$ colour matching function has been used as the single underlying sensor. Under CIE illuminants $D65$ and A (spectral power distributions $p_{D65}(\lambda)$ and $p_A(\lambda)$) the spectral weighting functions of the corresponding colour mechanisms are then $p_{D65}(\lambda)\bar{x}(\lambda)$ for φ_1, and $p_A(\lambda)\bar{x}(\lambda)$ for ψ_1.

For a given colour signal z obtained under $D65$, finding the metamer mismatch volume means determining the set of possible colour signals z' arising under A whose corresponding reflectances would be metameric to z under $D65$. The shaded region in Figure 1 shows $\Upsilon(\mathcal{X})$. Any point (z, z') inside $\Upsilon(\mathcal{X})$ represents the corresponding colour signals that would arise from a given object under illuminants $D65$ and A. As can be seen from the figure, using $z = 35$ as an example, all points (z, z') on the vertical line $z = 35$ and lying within the shaded area arise from objects that are metameric under $D65$ and also result in colour signal z' under A. Hence the z' values from the vertical line segment lying within the shaded area make up the metamer mismatch volume for the colour signal $z = 35$ under $D65$. In this example, the 'volume' degenerates to a line segment on the vertical (z') axis. The boundary of the volume is given by the z' values at the intersections of the $z = 35$ line with the boundary of $\Upsilon(\mathcal{X})$ (i.e., $z' = 20.5$ and $z' = 58$).

The situation is analogous for a trichromatic colour device, but $\Upsilon(\mathcal{X})$ becomes 6-dimensional and the cross-section is defined by the intersection of a 3-dimensional affine subspace with the boundary of $\Upsilon(\mathcal{X})$. In the general n-dimensional case, determining the metamer mismatch volume (denoted as $\mathcal{M}(\mathbf{z}_0; \Phi, \Psi)$) associated with the colour signal $\mathbf{z}_0 = \Phi(x_0)$ when switching from colour map Φ to colour map Ψ means determining its boundary, denoted $\partial\mathcal{M}(\mathbf{z}_0; \Phi, \Psi)$. Consider also the boundary of the $2n$-dimensional object-colour solid $\Upsilon(\mathcal{X})$, denoted $\partial\Upsilon(\mathcal{X})$. The boundary $\partial\mathcal{M}(\mathbf{z}_0; \Phi, \Psi))$ is determined by intersecting $\Upsilon(\mathcal{X})$ with the n-dimensional affine subspace containing $\mathbf{z}_0 = \Phi(x_0)$.

The object-colour solid, $\Upsilon(\mathcal{X})$, is determined by its boundary, $\partial\Upsilon(\mathcal{X})$, which in turn is fully specified by those objects that map to the boundary. In the colour literature reflectances mapping to the color-solid boundary are called *optimal* [1]. A method of evaluation of the optimal reflectances has been described elsewhere [2], [13]. Similarly, the metamer mismatch volume $\mathcal{M}(\mathbf{z}_0; \Phi, \Psi)$ is fully determined by its boundary, $\partial\mathcal{M}(\mathbf{z}_0; \Phi, \Psi)$. In this report we present a theoretical method and its computational implementation that for the first time provides a means of determining the reflectances that map to the mismatch volume boundary. We will refer to such reflectances as *μ-optimal with respect to* $\mathcal{M}(\mathbf{z}_0; \Phi, \Psi)$, or just *$\mu$-optimal* when it is clear which metamer mismatch volume is meant.

Let us denote the set of optimal reflectances for $\Upsilon(\mathcal{X})$ as $O(\Upsilon)$. Given a $\mathbf{z}_0$ in the Φ-subspace, $\partial\mathcal{M}(\mathbf{z}_0; \Phi, \Psi)$ will be defined by the Ψ-images of those optimal reflectances $x_{opt} \in O(\Upsilon)$ satisfying the following equation:

$$\Phi(x_{opt}) = \mathbf{z}_0. \tag{3}$$

In other words, all the optimal reflectances satisfying this equation will be μ-optimal, that is, they will be mapped by Ψ to the boundary of the metamer mismatch volume:

$$\partial\mathcal{M}(\mathbf{z}_0; \Phi, \Psi) = \{\mathbf{z}' = \Psi(x_{opt}) : \Phi(x_{opt}) = \mathbf{z}_0.\}$$

It is not possible to solve this equation directly because the set of possible optimal reflectances is infinite. However, optimal reflectances $O(\Upsilon)$ lend themselves to finite parameterisation [2], [13]. The possibility of such parameterisation emerges from the fact that the optimal reflectances are step-like functions that can be characterized by a finite number of transition wavelengths.

Historically, Schrödinger was the first to claim that the optimal spectral reflectance functions can take only two values: either 0 or 1 [14]. Moreover, he conjectured that for human colour vision the optimal spectral reflectance functions have

Copyright (c) 2013 IEEE. Personal use is permitted. For any other purposes, permission must be obtained from the IEEE by emailing pubs-permissions@ieee.org.

This is the author's version of an article that has been published in this journal. Changes were made to this version by the publisher prior to publication.
The final version of record is available at http://dx.doi.org/10.1109/TIP.2013.2283148

the form of elementary step functions. Following the terminology accepted by other authors [2], [13], [15], functions

$$x_m(\lambda;\lambda_1,...,\lambda_m)=\sum_{i=1}^{m}(-1)^{i-1}x_1(\lambda;\lambda_i) \tag{4}$$

and

$$1-x_m(\lambda;\lambda_1,...,\lambda_m),$$

where

$$x_1(\lambda;\lambda_1)=\begin{cases}0, & \text{if} \quad \lambda<\lambda_1\\ 1, & \text{if} \quad \lambda\geq\lambda_1;\end{cases} \tag{5}$$

$\lambda_{\min}<\lambda_1<\lambda_2<...<\lambda_m<\lambda_{\max}$, are called the *elementary step functions of type* m, with $\lambda_1,...,\lambda_m$ being referred to as *transition wavelengths*.

Schrödinger believed that for human vision the optimal spectral reflectance functions were of type $m<3$. However, this is not correct. As pointed out by some other researchers [13], [15], [16], the number of transition wavelengths may exceed the number of the colour mechanisms. More generally, a theorem has been proved by a Russian mathematician, Vladimir Levin, showing that for a colour map Φ based on colour mechanisms having continuous spectral weighting functions $s_1(\lambda),...,s_n(\lambda)$, an elementary step function with transition wavelengths $\lambda_1,...,\lambda_m$ will be an optimal spectral reflectance function if $\lambda_1,...,\lambda_m$ are the only zero-crossings of the following equation [2]:

$$k_1s_1(\lambda)+k_2s_2(\lambda)+...+k_ns_n(\lambda)=0, \tag{6}$$

where $k_1,k_2,...,k_n$ are arbitrary real numbers (at least one of which is not equal to zero). We would like to emphasize that while we use this theorem in the development of our algorithm, the tests described later in the paper verify that the algorithm works without relying on the theorem as proof.

It also follows that the perfect reflector and the perfect absorber[3] are optimal reflectances. Formally, they correspond to the case when Eq. 6 has no zero-crossings [2].

Given another colour map Ψ with continuous spectral weighting functions $s'_1(\lambda),...,s'_n(\lambda)$ and combining it with Φ to form the colour map Υ, the zero-crossings of the equation

$$k_1s_1(\lambda)+...+k_ns_n(\lambda)+k'_1s'_1(\lambda)+...+k'_ns'_n(\lambda)=0 \tag{7}$$

will determine an optimal spectral reflectance function with respect to Υ. Let us designate this optimal reflectance $x(\lambda;\mathbf{k},\mathbf{k}')$, where $\mathbf{k}=(k_1,...,k_n)$, and $\mathbf{k}'=(k'_1,...,k'_n)$.

Now consider an arbitrary reflectance x_0 mapping to colour signal $\mathbf{z}_0=\Phi(x_0)$ that lies in the interior[4] of the object-colour solid $\Phi(\mathcal{X})$. Then $\partial\mathcal{M}(\mathbf{z}_0;\Phi,\Psi))$ in the object-colour solid $\Psi(\mathcal{X})$ will be implicitly defined by the following equation with respect to $\mathbf{k}$ and $\mathbf{k}'$:

$$\Phi(x(\lambda;\mathbf{k},\mathbf{k}'))=\mathbf{z}_0. \tag{8}$$

As $\mathbf{z}_0$ is an interior point, $\mathbf{k}'$ cannot equal zero, since if $\mathbf{k}'=0$ $x(\lambda;\mathbf{k},\mathbf{k}')$ is an optimal spectral reflectance function with respect to Φ, and thus $\Phi(x(\lambda;\mathbf{k},\mathbf{k}'))$ would be on the Φ-object-colour-solid boundary.

Let us consider the particular situation when $n=3$. In this case, given $\mathbf{z}_0=(z_1,z_2,z_3)$, Eq. 8 can be expanded as:

$$\begin{aligned}\varphi_1(x(\lambda;\mathbf{k},\mathbf{k}'))&=z_1,\\ \varphi_2(x(\lambda;\mathbf{k},\mathbf{k}'))&=z_2,\\ \varphi_3(x(\lambda;\mathbf{k},\mathbf{k}'))&=z_3.\end{aligned} \tag{9}$$

Denote the Ψ image of x_0 as $\mathbf{z}'_0=(z'_1,z'_2,z'_3)$, i.e., $\Psi(x_0)=\mathbf{z}'_0$, and let us introduce a polar coordinate system (ρ,β,γ) in the Ψ subspace with its origin at $\Psi(x_0)$. Let $x(\lambda;\mathbf{k},\mathbf{k}')$ satisfy Eq. 9. Then we have

$$\begin{aligned}\psi_1(x(\lambda;\mathbf{k},\mathbf{k}'))-z'_1&=\rho\cos\beta\sin\gamma,\\ \psi_2(x(\lambda;\mathbf{k},\mathbf{k}'))-z'_2&=\rho\sin\beta\sin\gamma,\\ \psi_3(x(\lambda;\mathbf{k},\mathbf{k}'))-z'_3&=\rho\sin\gamma.\end{aligned} \tag{10}$$

Note that if Eq. 7 admits a solution given vectors $\mathbf{k}$ and $\mathbf{k}'$ it will admit the same solution given vectors $\sigma\mathbf{k}$ and $\sigma\mathbf{k}'$, where σ is an arbitrary non-zero real number. Hence, we need only consider vectors $\mathbf{k}$ and $\mathbf{k}'$ such that the resultant vector $(\mathbf{k},\mathbf{k}')$ lies on the unit sphere in $\mathbf{R}^6$, that is,

$$\|(k_1,k_2,k_3,k'_1,k'_2,k'_3)\|_2=1. \tag{11}$$

Taken together, equations (9 - 11) define a two-dimensional manifold. Indeed, for each choice of β and γ, equations (9 - 11) can be resolved with respect to $k_1,k_2,k_3,k'_1,k'_2,k'_3$, and ρ. Furthermore, equations (9 - 11) implicitly define a function $\rho(\beta,\gamma)$ that determines the boundary $\partial\mathcal{M}(\mathbf{z}_0;\Phi,\Psi)$ induced by the point $\Phi(x_0)$. In other words, given β and γ, we have 7 equations in 7 unknowns. Resolving these equations one gets the location of the metamer mismatch volume's boundary in the direction (β, γ). Figure 2 illustrates the situation for a dichromatic sensor system.

Practical solution of equations (9 - 11) is complicated by the fact that different sets of $k_1,k_2,k_3,k'_1,k'_2,k'_3$ might determine the same optimal reflectance. For example, for the case of positive spectral weighting functions, Eq. 7 will have no roots when $k_1,...,k_n,k'_1,...,k'_n$ are either all positive, or all negative. Since the human spectral sensitivity functions are everywhere positive, all positive and all negative sets of $k_1,k_2,k_3,k'_1,k'_2,k'_3$ bring about the same two optimal reflectances: the perfect reflector and absorber. As these belong to the Φ-object-colour solid boundary $\partial\Phi(\mathcal{X})$ (i.e., they are not interior points in $\Phi(\mathcal{X})$), they need not be considered further. Hence, we see that parameterising the optimal reflectances in terms of $k_1,...,k_n,k'_1,...,k'_n$ is perhaps not the best approach.

We need a more convenient parameterisation of the optimal reflectances. We begin with the fact that Eq. 7 has a rather straightforward geometrical interpretation; namely, the roots of Eq. 7 are those wavelengths at which the spectral curve[5] intersects the hyperplane in $\mathbf{R}^{2n}$ passing through the origin and

[3]Perfect reflector (respectively absorber) takes the value 1 (respectively 0) for every wavelength in $[\lambda_{\min},\lambda_{\max}]$.

[4]It has been shown that for the colour mechanisms with positive spectral weighting functions the optimal reflectances have no metamers [2]. It follows that there is no metamer mismatching for the boundary points of the object-colour solid. In other words, the metamer mismatch volume for such points degenerates to a point. As such a case is of no interest, we exclude the boundary points from further consideration.

[5]In the $2n$-dimensional colour signal space determined by the colour mechanisms $(\varphi_1,...,\varphi_n,\psi_1,...,\psi_n)$, the curve $\overrightarrow{\sigma}(\lambda)=(\varphi_1(\delta(\mu-\lambda)),\varphi_2(\delta(\mu-\lambda)),\varphi_3(\delta(\mu-\lambda)),\psi_1(\delta(\mu-\lambda)),\psi_2(\delta(\mu-$ $(\lambda\in[\lambda_{\min},\lambda_{\max}])$ is called the *spectral curve*. Here $\delta(\mu-\lambda)$ stands for the Dirac delta function centered at wavelength λ.

Copyright (c) 2013 IEEE. Personal use is permitted. For any other purposes, permission must be obtained from the IEEE by emailing pubs-permissions@ieee.org.

This is the author's version of an article that has been published in this journal. Changes were made to this version by the publisher prior to publication.
The final version of record is available at http://dx.doi.org/10.1109/TIP.2013.2283148

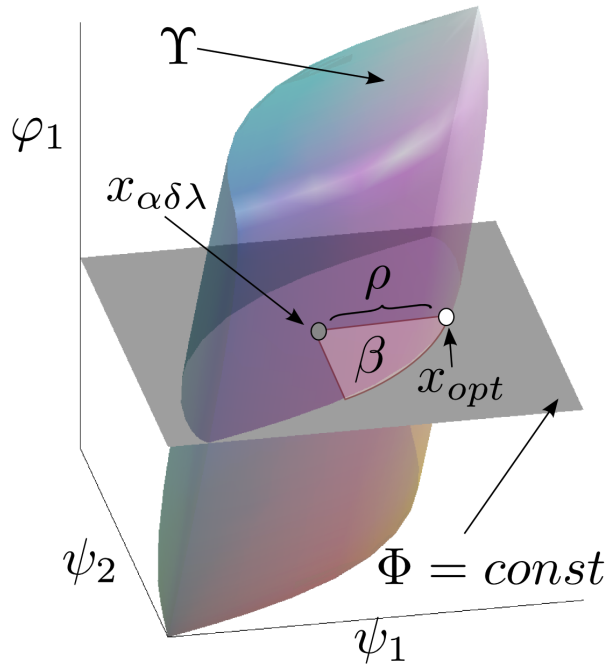

Figure 2. Illustration of the boundary of the metamer mismatch volume described by $\rho(\beta)$ relative to the origin $x_{\alpha\delta\lambda}$ for the case of a dichromatic system. Given two sets of colour mechanisms $\Phi = (\varphi_1, \varphi_2)$ and $\Psi = (\psi_1, \psi_2)$, then $\Upsilon(x) = (\varphi_1(x), \varphi_2(x); \psi_1(x), \psi_2(x))$. In the figure, only 3 of the 4 dimensions of the object-colour solid, $\Upsilon(\mathcal{X})$, are shown. For a given $\Phi = (\varphi_1, \varphi_2)$, the boundary of its metamer mismatch volume is determined by the intersection of the plane it defines and the boundary Υ. To describe that boundary, an origin for the polar coordinate system is situated at $x_{\alpha\delta\lambda}$ from which the metamer mismatch volume is represented in terms of polar angle β and distance ρ to points $x_{opt} = x_3(\lambda; \lambda_1, ..., \lambda_3)$ on the boundary of Υ. In this 4-dimensional case, the optimal functions on the boundary of Υ now are 3-transition functions. For a given β, the transition wavelengths of $\lambda, ..., \lambda_3$ of x_{opt} are found by optimization under the constraint that the resulting reflectance must lie on the plane defined by Φ.

determined by $k_1, ..., k_n, k'_1, ..., k'_n$. Indeed, any hyperplane in $\mathbf{R}^m$ through the origin is of the form $k_1 x_1 + ... + k_m x_m = 0$ where $x_1, ..., x_m$ are coordinates in $\mathbf{R}^m$, and the vector of the $k_1, ..., k_m$ coefficients uniquely defines the hyperplane. Therefore, if some λ_0 is a root of Eq. 7 it means that the point $(s_1(\lambda_0), ..., s_n(\lambda_0), s'_1(\lambda_0), ..., s'_n(\lambda_0))$ lies on the hyperplane determined by $k_1, ..., k_n, k'_1, ..., k'_n$.

Any $2n-1$ different wavelengths uniquely determine a hyperplane in $\mathbf{R}^{2n}$ through the origin that intersects the spectral curve at the points corresponding to these wavelengths (and perhaps also at some other points). When $n = 3$ the hyperplane in $\mathbf{R}^6$ is fully specified by 5 different wavelengths $\lambda_1, ..., \lambda_5$. The coefficients $k_1, k_2, k_3, k'_1, k'_2, k'_3$ of this hyperplane can be expressed as functions of these wavelengths $\lambda_1, ..., \lambda_5$.

Thus, each set of wavelengths $\lambda_1, ..., \lambda_5$ defines a hyperplane in $\mathbf{R}^6$ that intersects the spectral curve at wavelengths $\lambda_1, ..., \lambda_5$ and possibly at some other m wavelengths $\lambda_6, ..., \lambda_{5+m}$ as well. Considered as transition wavelengths, the set $\lambda_1, ..., \lambda_5, \lambda_6, ..., \lambda_{5+m}$ specifies an optimal reflectance (i.e., one that maps to the boundary $\partial\Upsilon(\mathcal{X})$ of the object-colour solid $\Upsilon(\mathcal{X})$). Since the addtional m wavelengths are uniquely determined by the first 5, the first 5 suffice as a parameterization of the optimal reflectances. Let us denote such an optimal reflectance as $x(\lambda; \lambda_1, ..., \lambda_5)$. If it satisfies Eq. 3 then it belongs to $\partial\mathcal{M}(\mathbf{z}_0; \Phi, \Psi)$. In other words, that optimal reflectance is on the boundary of the metamer mismatch volume. Hence, we again have a system of 6 equations in 6 unknowns similar to the equations in (9) and (10):

$$\begin{aligned}
\varphi_1(x(\lambda; \lambda_1, ..., \lambda_5)) &= z_1, \\
\varphi_2(x(\lambda; \lambda_1, ..., \lambda_5)) &= z_2, \\
\varphi_3(x(\lambda; \lambda_1, ..., \lambda_5)) &= z_3, \\
\psi_1(x(\lambda; \lambda_1, ..., \lambda_5)) - z'_1 &= \rho\cos\beta\sin\gamma, \\
\psi_2(x(\lambda; \lambda_1, ..., \lambda_5)) - z'_2 &= \rho\sin\beta\sin\gamma, \\
\psi_3(x(\lambda; \lambda_1, ..., \lambda_5)) - z'_3 &= \rho\sin\gamma.
\end{aligned} \tag{12}$$

Choosing β and γ defines a direction in the Φ subspace relative to the point (z_1, z_2, z_3). Solving equations (12) with respect to $\lambda_1, ..., \lambda_5$ and ρ yields the location of the boundary in the direction (β, γ).

Note that setting 2 of the 5 wavelengths $\lambda_1, ..., \lambda_5$ to be $\lambda_{\min}$ and $\lambda_{\max}$ while varying the other 3, we obtain all the optimal reflectances (if any) having 3 or 4 transition wavelengths, rather than 5. Generally, there might also exist optimal reflectances (for the object-colour solid $\Upsilon(\mathcal{X})$) with fewer than 3 wavelength transitions. However, most of them map to the Φ-object-colour-solid boundary. As we consider only internal points $\mathbf{z}_0$ in $\Phi(\mathcal{X})$, only a small fraction of the optimal reflectances with 1 and 2 transition wavelengths can be potentially μ-optimal; and an even smaller fraction of those—namely the ones satisfying the first 3 equations in (12)—will indeed be μ-optimal. Therefore, solving equations (12) we will obtain virtually all the points on $\partial\mathcal{M}(\mathbf{z}_0; \Phi, \Psi)$. If one does not want to risk missing even a small fraction of the points on $\partial\mathcal{M}(\mathbf{z}_0; \Phi, \Psi)$, then one has to resort to solving equations (9 - 11) which guarantees, in theory, no loss of μ-optimal reflectances at all.

III. Calculating Metamer Mismatch Volumes

Let us apply this theory to the problem of evaluating the metamer mismatch volumes induced for the CIE 1931 standard observer when moving from CIE illuminant $D65$ to CIE illuminant A. In this case, Equation 7 takes the form

$$\begin{aligned}
&(k_1 s_1(\lambda) + k_2 s_2(\lambda) + k_3 s_3(\lambda)) p_{D65}(\lambda) \\
&+ (k'_1 s_1(\lambda) + k'_2 s_2(\lambda) + k'_3 s_3(\lambda)) p_A(\lambda) = 0
\end{aligned} \tag{13}$$

where $s_1(\lambda), s_2(\lambda)$ and $s_3(\lambda)$ are the CIE 1931 colour matching functions, and $p_{D65}(\lambda)$ and $p_A(\lambda)$ are the spectral power distributions for CIE illuminants $D65$ and A.

For the CIE 1931 colour matching functions, the optimal reflectances turn out to be elementary step functions of type $m < 3$, in accord with Schrödinger's conjecture [13], [16]. Yet, the optimal stimuli for the 6-dimensional Υ-object-colour solid are not necessarily elementary step functions of type $m < 6$. In other words, random choices of the 5 transition wavelengths might lead to solutions to equation (12) with more than 5 roots.

It follows that if one uses only the elementary step functions of type $m \leq 5$ (let us denote these $\mathcal{O}_5$) one will get only an approximation to the full 6-dimensional object-colour solid

Copyright (c) 2013 IEEE. Personal use is permitted. For any other purposes, permission must be obtained from the IEEE by emailing pubs-permissions@ieee.org.

This is the author's version of an article that has been published in this journal. Changes were made to this version by the publisher prior to publication.
The final version of record is available at http://dx.doi.org/10.1109/TIP.2013.2283148

$\Upsilon(\mathcal{X})$. More formally, given a colour map $\digamma : \mathcal{X} \rightarrow \mathbf{R}^n$, and the set of all the elementary step functions of type $m < n$ (written as $\mathcal{O}_n$), let us call the volume confined by $\digamma(\mathcal{O}_n)$ an *(n-1)-transition approximation* to $\digamma(\mathcal{X})$. The 2-transition approximation to the 3-dimensional object-colour solid based on the cone photopigment spectral sensitivities was found to deviate by not more than 1% from the true object-colour solid when measured along any direction from the object-colour solid's center [13]. In many computational tasks such deviation can be neglected. Although we have not evaluated the difference between $\Upsilon(\mathcal{X})$ and its 5-transition approximation, we decided to use the latter when computing the metamer mismatch volumes since this made our computations much simpler. Obviously, intersecting the 5-transition approximation to $\Upsilon(\mathcal{X})$ with the corresponding affine 3-dimensional subspace through $\mathbf{z}_0$ will produce a volume (denoted $\mathcal{M}_5(\mathbf{z}_0;\Phi,\Psi)$) lying inside the metamer mismatch volume $\mathcal{M}(\mathbf{z}_0;\Phi,\Psi)$. Let us call it the *5-transition approximation* to $\mathcal{M}(\mathbf{z}_0;\Phi,\Psi)$.

Given a point $\mathbf{z}_0 = (z_1, z_2, z_3)$ in the object-colour solid $\Phi(\mathcal{X})$, the boundary of the 5-transition approximation to the metamer mismatch volume $\mathcal{M}(\mathbf{z}_0;\Phi,\Psi)$ (denoted as $\partial\mathcal{M}_5(\mathbf{z}_0;\Phi,\Psi)$) in the object-colour solid $\Psi(X)$ is implicitly defined by the following equations with respect to the transition wavelengths $\lambda_1, ..., \lambda_5$:

$$\begin{aligned}
\varphi_1(x_5(\lambda;\lambda_1,...,\lambda_5)) &= z_1, \\
\varphi_2(x_5(\lambda;\lambda_1,...,\lambda_5)) &= z_2, \\
\varphi_3(x_5(\lambda;\lambda_1,...,\lambda_5)) &= z_3, \\
\psi_1(x_5(\lambda;\lambda_1,...,\lambda_5)) - z_1' &= \rho\cos\beta\sin\gamma, \\
\psi_2(x_5(\lambda;\lambda_1,...,\lambda_5)) - z_2' &= \rho\sin\beta\sin\gamma, \\
\psi_3(x_5(\lambda;\lambda_1,...,\lambda_5)) - z_3' &= \rho\sin\gamma,
\end{aligned} \tag{14}$$

where $x_5(\lambda;\lambda_1,...,\lambda_5)$ is an elementary step function of type $m = 5$. The difference between equations (14) and (12) is that (14) involves an elementary step function with the transition wavelengths $\lambda_1, ..., \lambda_5$, whereas (12) involves an elementary step function that potentially has more than 5 transition wavelengths, but specifically including $\lambda_1, ..., \lambda_5$. The additional transition wavelengths can be determined by finding all the intersections of the spectral curve $\overrightarrow{\sigma}(\lambda)$ with the hyperplane defined by the origin and the five points on the spectral curve $\overrightarrow{\sigma}(\lambda_1), ..., \overrightarrow{\sigma}(\lambda_5)$ determined by $\lambda_1, ..., \lambda_5$.

IV. Matlab Implementation Details

The following describes one approach that has been implemented in Matlab to calculate the metamer mismatch volumes. In fact, any method of solving equations (14) will suffice. To solve equations (14) for $\rho(\beta,\gamma)$, we need to choose the origin of the polar coordinate system so as to define β,γ, and ρ. Although not strictly necesssary, it is preferable to choose an origin that belongs to, or better still lies inside, the metamer mismatch volume. When the point $\mathbf{z}_0$ is specified as the Φ colour signal of some known reflectance, say, x_0, then the Ψ-image of x_0 lends itself as a natural choice for the origin. When the point $\mathbf{z}_0$ is given simply as some Φ colour signal (without relating it to any reflectance), choosing a point inside the metamer mismatch volume might appear to be somewhat more problematic since we do not yet know what that volume is. However, any reflectance that is metameric to $\mathbf{z}_0$ under Φ will suffice.

To find a metamer to $\mathbf{z}_0$ we make use of a rectangular metamer of the kind introduced by Logvinenko (2009) [13]. For any given point $\mathbf{z}_0 = (z_1, z_2, z_3)$ in the object-colour solid, $\Phi(\mathcal{X})$, its rectangular metamer is defined as a rectangular reflectance spectrum that is a linear combination of an elementary step function of type $m < 3$ and $x_{0.5}(\lambda) = 0.5$. As the rectangular metamer is specified by three numbers—α, δ and λ—it will be denoted as $x_{\alpha\delta\lambda}$ (for more detail see Logvinenko, 2009). To find the rectangular metamer for $\mathbf{z}_0$ the code of Godau et al. [17], [18] is used. The resulting rectangular metamer $x_{\alpha\delta\lambda}$ is by construction metameric to $\mathbf{z}_0$. Therefore, the point $\Psi(x_{\alpha\delta\lambda})$ is guaranteed to be in the metamer mismatch volume. Although highly unlikely, $\Psi(x_{\alpha\delta\lambda})$ could potentially belong to the metamer mismatch volume boundary, and therefore not lie strictly inside the mismatch volume. As such, it would be an unsuitable choice for the origin (z_1', z_2', z_3') of the polar coordinate system. To ensure that we have a point strictly inside the metamer mismatch volume, we take an arbitrary point on its boundary and then use the midpoint between it and $\Psi(x_{\alpha\delta\lambda})$ as the origin.

Determining $\rho(\beta,\gamma)$ proceeds in two steps. Given (β,γ) the first step is the more difficult one and involves finding the optimal 5-transition step function $x_{opt} = x_5(\lambda;\lambda_1,...,\lambda_5)$ metameric to $\mathbf{z}_0$ such that $\Psi(x_5(\lambda;\lambda_1,...,\lambda_5))$ lies in the direction defined by (β,γ). The second step is then simply to calculate ρ directly using x_{opt} from the first step.

To accomplish the first step we minimized the following objective function formed as the sum of two error measures,

$$E(x_{opt}) = E_\Phi(x_{opt}) + E_{\Psi\beta\gamma}(x_{opt}).$$

The first term corresponds to the constraints provided by equations 14 and is

$$E_\Phi(x_{opt}) = \|\Phi(x_{opt}) - \mathbf{z}_0\|.$$

The second term ensures that the 5-transition reflectance lies in the desired direction under Ψ and is defined by

$$E_{\Psi\beta\gamma}(x_{opt}) = \arccos\left(\frac{\hat{u}\cdot(\Psi(x_{opt}) - \mathbf{z}_0')}{\|\Psi(x_{opt}) - \mathbf{z}_0'\|}\right),$$

where $\hat{u} = (sin(\beta)cos(\gamma), sin(\beta)sin(\gamma), cos(\beta))$ is the unit vector in the direction given by (β,γ). Once x_{opt} has been found, ρ can be directly calculated as

$$\rho = \|\Psi(x_{opt}) - \Psi(x_0)\|.$$

The above method means that $\partial\mathcal{M}_5(\mathbf{z}_0;\Phi,\Psi)$ (i.e., the boundary of the 5-transition approximation to the metamer mismatch volume $\mathcal{M}(\mathbf{z}_0;\Phi,\Psi)$) can be precisely computed as the distance $\rho(\beta,\gamma)$ from the chosen origin (z_1', z_2', z_3') to the boundary in any given direction as specified by the angles β and γ. To model the entire boundary, one possibility is to step through values of β and γ and thereby obtain a regular sampling of the boundary. However, such an approach is rather time-consuming. In order to speed up computation when preparing the data for the present report, we produced a large number of random points over $\partial\Upsilon(\mathcal{O}_5)$ (i.e., the boundary

Copyright (c) 2013 IEEE. Personal use is permitted. For any other purposes, permission must be obtained from the IEEE by emailing pubs-permissions@ieee.org.

This is the author's version of an article that has been published in this journal. Changes were made to this version by the publisher prior to publication.
The final version of record is available at http://dx.doi.org/10.1109/TIP.2013.2283148

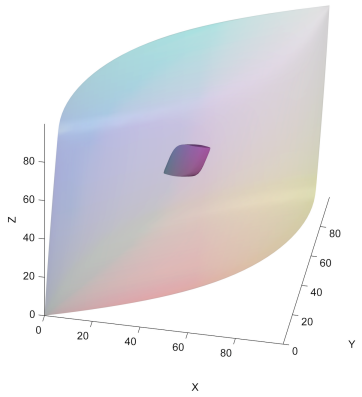

Figure 3. Metamer mismatch volume arising at the centre of the object-colour solid for the flat grey reflectance for a change of illumination from $D65$ to A. The coordinate axes are the CIE XYZ.

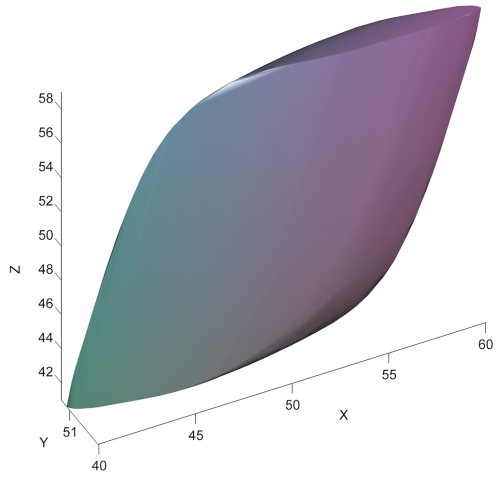

Figure 4. Expanded view of the metamer mismatch volume for the case of the flat grey reflectance shown in Figure 3.

of the 5-transition approximation to $\Upsilon(\mathcal{X})$) by generating random 5-transition reflectances $x_{opt} = x_5(\lambda; \lambda_1, ..., \lambda_5)$ and then selected only those that minimize $\|\Phi(x_{opt}) - z_0)\|$. This eliminates the angular term involved in $E_{\Psi\beta\gamma}(x_{opt})$ and significantly speeds up the calculation, but has the disadvantage that the resulting points are not systematically distributed over the boundary $\partial\mathcal{M}_5(\mathbf{z}_0; \Phi, \Psi)$. It should be borne in mind that such an approach differs from that of previous authors in that we generated reflectances metameric to x_{opt} that belonged not just to the colour solid $\Phi(\mathcal{X})$ but to the boundary $\partial\mathcal{M}_5(\mathbf{z}_0; \Phi, \Psi)$. For this reason our selected reflectances are restricted to belonging to the boundary of the 5-transition approximation to the metamer mismatch volume $\partial\mathcal{M}(\mathbf{z}_0; \Phi, \Psi)$ rather than belonging to the full metamer mismatch volume (most likely inside it), as is the case for the methods described in previous studies.

V. Examples

The Matlab implementation provides the opportunity to explore the true potential extent of metamer mismatching for the first time. Consider the simple case of a flat grey reflectance under illuminant $D65$ versus A. Figure 3 shows the 5-transition approximation to the metamer mismatch volume arising at the centre of the object-colour solid (i.e., for $\Phi(x_{0.5}(\lambda))$ where $x_{0.5}(\lambda) = 0.5$, the flat grey reflectance) for the CIE 1931 2-degree standard observer when the illumination changes from $D65$ to A. Interestingly, its shape (Figure 4) roughly resembles that of the object-colour solid. The 5-transition approximation $\mathcal{M}_5(\Phi(x_{0.5}(\lambda)); \Phi, \Psi)$ is clearly elongated. [6] Figure 5 depicts the same volume (i.e., $\mathcal{M}_5(\Phi(x_{0.5}(\lambda)); \Phi, \Psi)$) in colour opponent coordinates based on the Smith & Pokorny cone fundamentals. From this figure it is clear that $\mathcal{M}_5(\Phi(x_{0.5}(\lambda)); \Phi, \Psi)$ is elongated along the (S-(L+M)) axis which is believed to be associated with the

[6]The 5-transition reflectances used in this and all similar figures in the paper are available for download from "http://www.cs.sfu.ca/∼colour/data/". Using the reflectances, the reader can generate similar figures from various viewpoints, and also confirm that they are all metameric under the first illuminant.

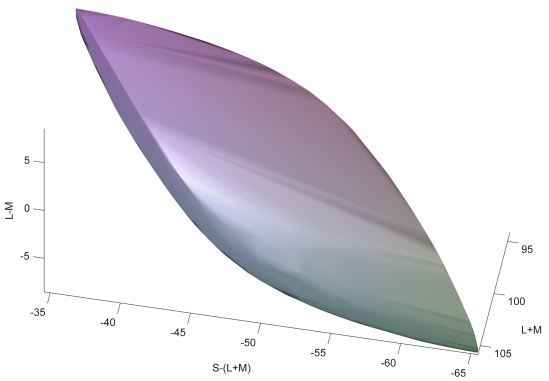

Figure 5. Metamer mismatch volume for the flat grey reflectance for a change of illumination from D65 to A. The coordinate axes are the Smith-Pokorny cone fundamentals transformed to opponent color axes.

yellow-blue mechanism [19], [20]. Therefore, the metamers looking achromatic under illuminant $D65$ disperse mainly along the yellow-blue axis under illuminant A. This agrees with our intuition since illuminant A appears more yellowish than $D65$.

Metamer mismatching can be surprisingly dramatic in that it can disperse flat grey into a full hue circle of different hues. For example, Figure 6 shows a circle of hues falling on the boundary of the metamer mismatch volume of flat grey for the case of the lighting changing from a green to a neutral ("white") illuminant (see reference [21] for the green and neutral spectra). In other words, these are the hues of 20 reflectances as they would be seen under the neutral light. Needless to say, the figure here reproduces the exact hues only approximately. Despite the fact that these 20 reflectances appear so varied in hue under the neutral light, they are, in fact, all metameric to one another, as well as to flat grey, under the green light. Not only does this example have implications

Copyright (c) 2013 IEEE. Personal use is permitted. For any other purposes, permission must be obtained from the IEEE by emailing pubs-permissions@ieee.org.

This is the author's version of an article that has been published in this journal. Changes were made to this version by the publisher prior to publication.
The final version of record is available at http://dx.doi.org/10.1109/TIP.2013.2283148

for human colour perception, as discussed by Logvinenko et al. [7], [8] it also has consequences for image processing and machine vision since it shows that the 'colour' of an object is not a stable, intrinsic feature since one colour can potentially become many very different colours.

Each reflectance underlying the hue circle is a 5-transition reflectance from the boundary of the metamer mismatch volume for flat grey. The transition wavelengths for each reflectance are listed in Table II. Each reflectance is 0 from $\lambda_{\min} = 380$ nm to the first transition wavelength at which point it becomes 1 until the second transition wavelength and so on until $\lambda_{\max} = 780$. Table II also lists the XYZ values of the 20 5-transition reflectances illuminated by the green light. Clearly, they are metameric with high precision, which they need to be since it would otherwise imply a flaw in the Matlab implementation.

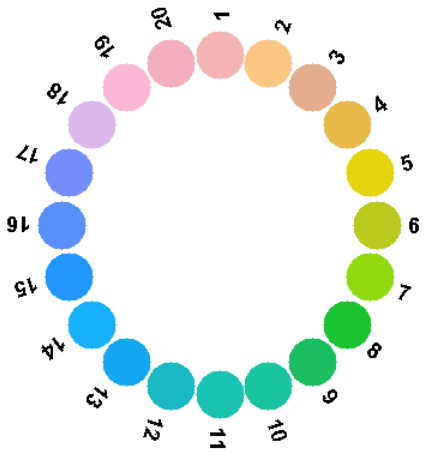

Figure 6. Hue circle of 5-transition reflectances shown illuminated by the neutral light N. These reflectances are, in fact, all metameric to flat grey under the green light.

T1	T2	T3	T4	T5	X	Y	Z
453.8	493.0	519.6	542.7	568.0	16.81584	50.0002	8.16469
381.3	443.7	494.3	528.7	555.8	16.81582	50.0001	8.16467
464.1	499.0	526.1	550.1	579.0	16.81574	49.9999	8.16467
479.8	509.1	530.3	551.6	577.0	16.81579	50.0000	8.16468
491.0	528.1	555.3	640.7	696.9	16.81582	50.0001	8.16467
490.0	525.6	551.2	582.5	603.8	16.81575	50.0000	8.16469
607.8	554.7	527.7	490.8	388.0	16.81577	50.0000	8.16468
487.5	520.3	544.2	570.4	631.6	16.81577	50.0000	8.16467
567.4	541.8	518.2	487.6	431.4	16.81577	50.0000	8.16467
583.2	551.1	526.0	494.7	450.3	16.81576	49.9999	8.16468
582.0	550.8	525.9	495.9	454.7	16.81575	50.0000	8.16470
574.8	547.6	523.9	496.1	458.3	16.81582	50.0000	8.16469
566.2	542.2	521.3	502.2	474.0	16.81577	50.0000	8.16468
579.4	553.0	531.2	509.5	480.0	16.81578	50.0000	8.16469
602.1	591.6	553.9	527.3	490.7	16.81578	50.0001	8.16469
431.6	492.2	528.2	555.3	623.2	16.81576	50.0000	8.16469
430.3	492.0	528.1	555.1	617.6	16.81576	50.0000	8.16470
628.4	558.4	532.3	505.7	473.9	16.81581	50.0001	8.16470
435.6	476.4	505.7	532.3	558.5	16.81579	50.0001	8.16470
452.4	493.6	521.7	545.2	571.4	16.81578	50.0001	8.16469

Table II
TRANSITION WAVELENGTHS OF THE 20 REFLECTANCES (ONE PER ROW), WHICH WERE USED IN CONSTRUCTING FIGURE 6, AND THEIR CORRESPONDING XYZ UNDER GREEN LIGHT. AS SHOWN IN FIGURE 6, THEY FORM A HUE CIRCLE UNDER NEUTRAL ("WHITE") LIGHT; NONETHELESS, THEY ARE ALL METAMERIC TO FLAT GREY UNDER THE GREEN LIGHT. ALTHOUGH THE TRANSITION WAVELENGTHS HAVE BEEN ROUNDED TO ONE DECIMAL PLACE, THE ENTRIES ARE BASED ON THE ORIGINAL, FULL PRECISION WAVELENGTH DATA AVAILABLE FOR DOWNLOAD FROM "HTTP://WWW.CS.SFU.CA/∼ COLOUR/DATA/" (***TYPESETTER: ALL LOWERCASE IN URL***)

Note that the final published version includes an explanation of how to use the numbers in this table.

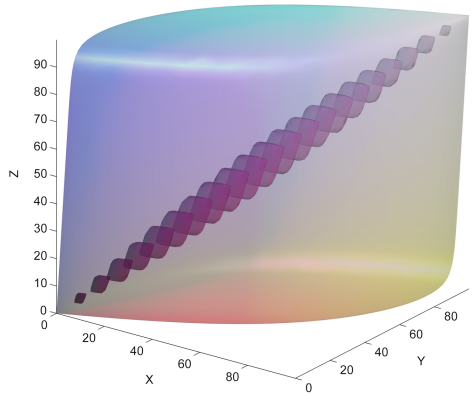

Figure 7. Metamer mismatch volumes for points lying along the achromatic interval connecting the black pole (origin) and white pole (apex furthest from origin) of the Ψ-object-colour solid. The maximum volume occurs at the center ($x_{0.5}$) and volumes decrease towards both poles. The metamer mismatch indices obtained at a finer sampling of locations along the achromatic interval are plotted in Figure 8.

VI. METAMER MISMATCH INDEX

To quantify the degree of metamer mismatching occurring for a given point in the Φ colour space, we introduce a *metamer mismatch index*. The metamer mismatch index $i_{mm}(\mathbf{z}_0; \Phi, \Psi)$ of the metamer mismatching for a point $\mathbf{z}_0$ in the Φ-object-colour solid induced by a change in the colour mechanisms from Φ to Ψ is defined as a ratio of volumes:

$$i_{mm}(\mathbf{z}_0; \Phi, \Psi) = \frac{v(\mathcal{M}(\mathbf{z}_0; \Phi, \Psi))}{v(\Psi(\mathcal{X}))}, \qquad (15)$$

where $v(\mathcal{M}(\mathbf{z}_0; \Phi, \Psi))$ is the volume of $\mathcal{M}(\mathbf{z}_0; \Phi, \Psi)$, and $v(\Psi(\mathcal{X}))$ is the volume of the Ψ-object-colour solid. Note that this index is invariant with respect to any non-singular linear transformation of the colour mechanisms Ψ.

Figure 7 shows the metamer mismatch volumes for a number of points lying along the achromatic interval connecting the black and white poles of the Φ-object-colour solid. The volumes clearly become smaller the closer they are to the poles. This is hardly surprising since there is known to be no metamerism on the object-colour solid boundary [2]. Figure 8 plots the metamer mismatch index (15) as a function of position along the achromatic axis from black to white.

VII. METAMER MISMATCH AREAS IN THE CHROMATICITY DIAGRAM

Metamer mismatching can be split into two components: chromaticity mismatching and luminance mismatching. The chromaticity mismatching component can be represented by

Copyright (c) 2013 IEEE. Personal use is permitted. For any other purposes, permission must be obtained from the IEEE by emailing pubs-permissions@ieee.org.

This is the author's version of an article that has been published in this journal. Changes were made to this version by the publisher prior to publication.
The final version of record is available at http://dx.doi.org/10.1109/TIP.2013.2283148

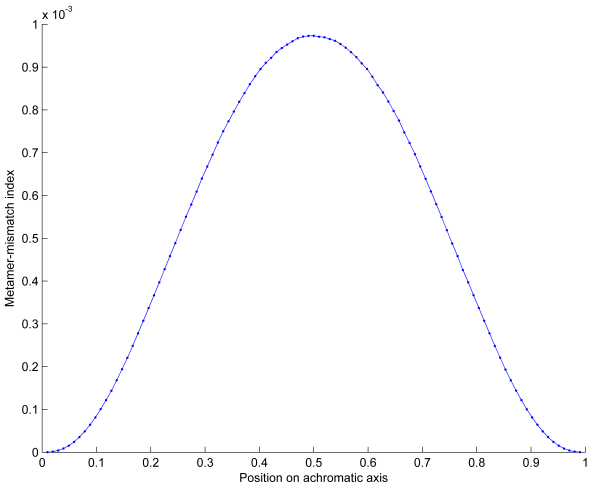

Figure 8. Metamer mismatch indices (Equation 15) plotted as a function of relative position along the achromatic interval (see Figure 7) from the black pole to the white pole.

projecting the metamer mismatch volume onto the chromaticity plane. This results in two-dimensional areas in the chromaticity plane showing the spread of chromaticities induced by a change of illuminant (or observer). Figure 9 presents the projection of the metamer mismatch volumes from Figure 7 onto the CIE 1931 xy-chromaticity plane. In chromaticity space, the smallest areas are near the white pole and the largest near the black pole, although in three-dimensions the volumes become small near both poles. One can see from Figure 7 that the solid angle from the origin subtended by the volumes near the black pole is clearly larger than that of the volumes further along the achromatic axis towards the white pole.

Presenting metamer mismatching in two dimensions can be advantageous in some situations. For example, if one is interested only in the metamer mismatching occurring in some plane in the Ψ-subspace, then there is no need to evaluate the entire metamer mismatch volume. Evaluating the boundary contours of the metamer mismatch areas in the given plane will suffice. This can be done by the addition of one equation to the method described above. In particular, given a polar coordinate system (ρ, β, γ) in the Ψ-subspace with its origin at $\Psi(x_{\alpha\delta\lambda})$, let

$$F(\beta, \gamma) = 0 \tag{16}$$

be an equation of the desired plane through $\Psi(x_{\alpha\delta\lambda})$. Fixing β (or γ) and solving equations (12) along with equation (16) with respect to $\lambda_1, ..., \lambda_5$, and ρ and γ (respectively β) yields a point on the metamer mismatch area boundary corresponding to the value β (respectively γ).

VIII. Conclusion

Metamer mismatching is an important aspect colour, whether in terms of digital colour imaging or human colour perception. It arises when the lighting changes, and also when the spectral sensitivity functions of one observer (or camera) differ from those of another. The metamer mismatch volume describes the set of colour signals that can arise under a change of light or observer. Previous methods of describing the metamer mismatch volume have all provided only approximations to the true volume. These methods probably provide good estimates of the true volume, but without knowing the true volume there is no way of knowing for sure. The results reported here provide a precise description of the true metamer mismatch volume in terms of its boundary. The method is general in that it applies for any reflectance lit by a strictly positive illuminant. The method is demonstrated via a Matlab program for computing metamer mismatch volumes. There are many practical applications for metamer mismatching theory and the associated code, which include better evaluation of the colour rendering properties of light sources, better evaluation of the colour accuracy of digital colour cameras, better rendering of printed or displayed colours, and a better understanding of what might or might not be possible in terms of providing a stable representation of the colour of objects under a change in illuminant.

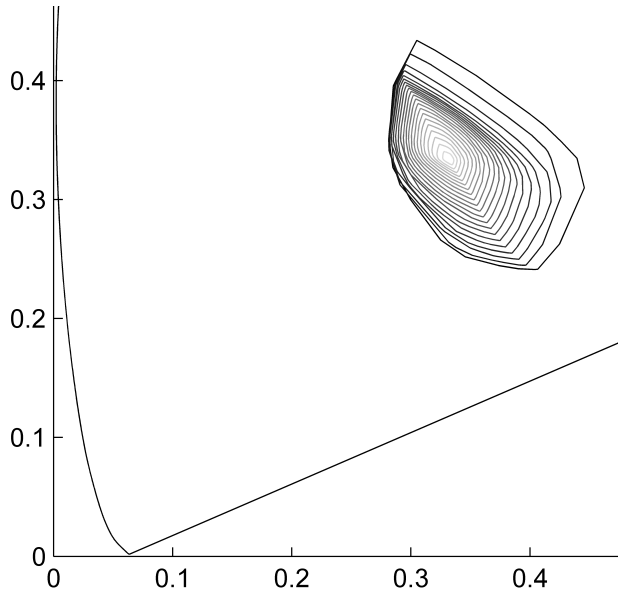

Figure 9. Projection into CIE 1931 xy-chromaticity space of the boundaries of the mismatch volumes shown in Figure 7 that occur along the achromatic axis. A portion of the spectral locus "horseshoe" is also shown. The largest area corresponds to the volume that lies closest to the black pole, the smallest one to the volume that lies closest to the white pole. This is in contrast to the corresponding 3-dimensional volumes for which the maximum volume occurs at the center ($x_{0.5}$) with size decreasing towards both poles.

Acknowledgment

Financial support was provided by the Natural Sciences and Engineering Research Council of Canada.

References

[1] G. Wyszecki and W. S. Stiles, *Color Science: Concepts and Methods, Quantitative Data and Formulae*, 2nd ed. New York: John Wiley and Sons, 1982.

Copyright (c) 2013 IEEE. Personal use is permitted. For any other purposes, permission must be obtained from the IEEE by emailing pubs-permissions@ieee.org.

This is the author's version of an article that has been published in this journal. Changes were made to this version by the publisher prior to publication.
The final version of record is available at http://dx.doi.org/10.1109/TIP.2013.2283148

[2] A. D. Logvinenko and V. L. Levin, "Foundations of colour science," *under review*, 2013.
[3] P. Urban and R. Grigat, "Metamer density estimated color correction," *Signal, Image and Video Processing*, July 2008.
[4] G. Finlayson and P. Morovic, "Metamer constrained color correction," *Journal of Imaging Science and Technology*, vol. 44, no. 4, pp. 295–, 2000.
[5] G. Finlayson and M. Drew, "Metamer sets and colour correction," *Journal of Image Science Technology*, 2000.
[6] G. Finlayson and P. Morovic, "Metamer constrained perceptual characterisation of digital cameras," in *Spring Conference on Computer Graphics (SCCG99)*. Budmerice, Slovakia: Association of Computing Machinery, 1999, pp. 21–22.
[7] A. D. Logvinenko, B. V. Funt, and H. Mirzaei, "The extent of metamer mismatching," in *Proceedings of the 12th Congress of the International Colour Association (AIC 2013)*. The Colour Group (GB), July 2013.
[8] ——, "Revisiting colour constancy," *under review*, (2013).
[9] J. Schanda, Ed., *Colorimetry*. New York: John Wiley and Sons, Inc., 2007.
[10] A. D. Logvinenko, "A new colour rendering index," in *Proceedings of the 11th Congress of the International Colour Association (AIC 2009). CD*, D. Smith, P. Green-Armytage, M. A. Pope, and N. Harkness, Eds. Sydney: Colour Society of Australia, 2009.
[11] G. D. Finlayson and P. Morovic, "Metamer sets," *J. Opt. Soc. Am. A*, vol. 22, no. 5, pp. 810–819, 2005.
[12] A. Stockman and L. T. Sharpe, "Spectral sensitivities," in *The senses: A comprehensive reference: Vol. 2. Vision*, T. D. Albright and R. H. Masland, Eds. San Diego: Academic press, 2007, pp. 87–100.
[13] A. D. Logvinenko, "An object-colour space," *Journal of Vision*, vol. 9, no. 11, Article 5, pp. 1–23, 2009.
[14] E. Schrödinger, "Theorie der Pigmente von grösster Leuchtkraft." *Annalen der Physik*, vol. 62, pp. 603–622, 1920.
[15] V. V. Maximov, *Transformatsii tsveta pri izmenenii osvescheniya*. Moscow: Nauka, 1984.
[16] G. West and M. H. Brill, "Conditions under which Schrodinger object colors are optimal," *Journal of the Optical Society of America*, vol. 73, pp. 1223–1225, 1983.
[17] C. Godau and B. Funt, "XYZ to ADL: Calculating Logvinenko's object color coordinates," in *Proc. Eighteenth IS&T Color Imaging Conference, San Antonio. Nov. 2010*. New Jersey, USA: Society of Imaging Science and Technology, 2010, pp. 334–339.
[18] ——, "The Logvinenko object color atlas in practice," *Color Research & Application*, vol. 37, pp. 117–125, 2012.
[19] L. M. Hurvich and D. Jameson, "An opponent-process theory of color vision," *Psychological Review*, vol. 64, pp. 384–404, 1957.
[20] P. K. Kaiser and R. M. Boynton, *Human Color Vision*, 2nd ed. Washington, DC: Journal of the Optical Society of America, 1996.
[21] A. D. Logvinenko and R. Tokunaga, "Colour constancy as measured by least dissimilar matching," *Seeing and Perceiving*, vol. 24, pp. 407–452, 2011.

Alexander Logvinenko received his B.S. in psychology (1972) and in applied mathematics (1979), and his Ph.D. in psychology (1974) from the Moscow State University, Russia. He worked in the Psychology Department of the Moscow State University (1975-1992), and at Queen's University of Belfast (1993-2004). Now he is Professor of Vision Sciences at the Glasgow Caledonian University. His research interests are in colour theory, colour vision, and psychophysics.

Brian Funt is Professor of Computing Science at Simon Fraser University where he has been since 1980. He obtained his Ph.D. from the University of British Columbia in 1976. His research focus is on computational approaches to modelling and understanding color.

Christoph Godau received his BS in physics (2008) from the Ruhr-University Bochum, Germany and his MS in colour science (2010) from the University of Saint-Etienne, France and the University of Eastern Finland. He is currently research engineer and Ph.D. candidate at Technische Universität Darmstadt, where he works on colorimetry and spectral imaging for industrial inspection systems.

Copyright (c) 2013 IEEE. Personal use is permitted. For any other purposes, permission must be obtained from the IEEE by emailing pubs-permissions@ieee.org.